Ecological Indicators 155 (2023) 111069

Contents lists available at ScienceDirect

Ecological Indicators

journal homepage: www.elsevier.com/locate/ecolind

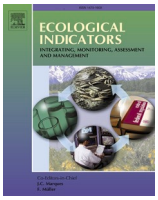

Future climate change accelerates the invasive rhythm of alien marine species: New insights into the invasive potential of the world's aquaculture species red drum *Sciaenops ocellatus*

Yongshuang Xiao [a,*], Jing Liu [a,*], Jiehong Wei [a], Zhizhong Xiao [a], Jun Li [a], Alfonso Aguilar-Perera [b], Angel Herrera-Ulloa [c]

[a] Center for Ocean Mega-Science, Institute of Oceanology, Chinese Academy of Sciences, Qingdao, China
[b] Departamento de Biología Marina, Facultad de Medicina Veterinaria y Zootecnia, Universidad Autónoma de Yucatán, Mexico
[c] Escuela de Ciencias Biológicas, Universidad Nacional, San José, Costa Rica

ARTICLE INFO

Keywords:
Sciaenops ocellatus
Invasion
species distribution model (SDM)
Stable isotope

ABSTRACT

In recent decades, an unprecedented frequency of red drum (*Sciaenops ocellatus*) escapes from sea cages (*i.e.*, million tail level) has generated enormous pressure on local marine biodiversity and ecosystems. This study aimed to assess the distribution and shifts of hotspot fitness zones for *S. ocellatus* under global climate change and to identify the trophic levels in the coastal waters of China. The species distribution model (SDM) identified four hotspot fitness zones at a global scale located in the Atlantic Ocean along the Gulf of Mexico and Uruguayan coasts, and in the Pacific Ocean along the Chinese and Australian coasts. Under global warming and climate change, the most suitable habitat for *S. ocellatus* would expand (448,178.6 km^2) and the centre of mass would shift northwards. Stable isotope $\delta^{15}N$ and $\delta^{13}C$ ratios indicated *S. ocellatus* has very high ecological competition, within a wide feeding range and high ecological position ($\delta^{15}N$: 10.84 ~ 12.84 ‰, 11.61 ± 0.62 ‰; $\delta^{13}C$: −15.28 ~ -17.25 ‰, −16.45 ± 0. 52 ‰) in the escape zone. The results suggested that a wide range of habitats, high reproductive capacity, and ecological niche competition conferred escaped *S. ocellatus* with a great ability to invade across regions on a global scale.

1. Introduction

Climate change and the introduction of non-native species have been identified as two major factors in global biodiversity loss (Bailey, 2015; Cowie, 1998; Gaither et al., 2013; Mack et al., 2000; McKinney and Lockwood, 1999; Pimentel et al., 2000; Sala et al., 2000), and the extent and significance of invasions are likely to increase with climate change and could interact in complex ways to further threaten native species (Dukes and Mooney, 1999; Hughes, 2000; Pimentel et al., 2005; Smith et al., 2000; Walther et al., 2009). Previous studies have found that invasive species were often more tolerant to changing environmental conditions than native species (Tatem et al., 2006) and might have a greater survival advantage as climate change progresses (Breitwisch, 2001; Padilla and Williams, 2004; Williamson and Fitter, 1996). Global agriculturalization is one of the most important ways to introduce exotic species into a new environment. These species have a visible economic value, but also have a major impact on the environment and human life (Ju et al., 2019; Kang et al., 2017; Kang et al., 2022). With the accelerated globalization of farmed species in recent years, the invasion of exotic species has not only threatened the survival of native fauna, but also may lead to serious degradation of terrestrial, marine, and freshwater ecosystems (Cuthbert et al., 2021; Geraldi et al., 2019; Kang et al., 2022; Luque et al., 2014). Aquatic ecosystems worldwide are currently suffering from substantial biodiversity loss and are highly susceptible to the combined effects of climate change and invasive species (Forrest and Taylor, 2002; Hill, 2009; Kang et al., 2022; Luque et al., 2014). For many invasive species, particularly marine invasive species, clear evidence of impacts was often lacking, even for those species considered to be significant threats (Blossey, 1999; Forrest and Taylor, 2002; Parker et al., 1999; Peterson, 1993).

The red drum, *Sciaenops ocellatus*, an estuarine fish, native to the western Atlantic Ocean from Massachusetts in the USA to northern Mexico, is one of the most important farmed fish worldwide (Ackerly et al., 2022; Bacheler et al., 2012; Forsberg et al., 1996; Rooker et al.,

* Corresponding authors.
E-mail addresses: dahaishuang1982@163.com (Y. Xiao), jliu@qdio.ac.cn (J. Liu).

https://doi.org/10.1016/j.ecolind.2023.111069
Received 20 May 2023; Received in revised form 21 August 2023; Accepted 9 October 2023
Available online 11 October 2023

2010; Watson et al., 2014). *S. ocellatus* was a broad-temperature and broad-salinity fish with a fast growth rate (≥10 °C, ~ 40 kg with wild-caught in the US), mixed feeding habits, high reproductive capacity (~2 million eggs/time), disease resistance, high survival rate (2 ~ 33 °C) and low oxygen tolerance (≥2.2 mg/l) (Craig et al., 1995; Jin et al., 2008; Thresher and Kuris, 2004; Xue, 2008). Therefore, *S. ocellatus* could not only quickly adapt to the bay, intertidal, and saline environments, but also even survive in inland freshwater areas (Bacheler et al., 2012; Jin et al., 2008; Rooker et al., 2010; Watson et al., 2014; Xue, 2008). The *S. ocellatus* fishery industry has gone through three important stages in its development from local fishery capture to global farming of the species: (1) the declining stage of fishing-based fisheries (1950 ~ 1981, CP: 35,973 ton), (2) the nascent stage of global farming (1982 ~ 1996, AQ: 76 ton, CP: 248 ton), and (3) the rapid development of global farming (1997 ~ 2019, AQ: 1,012,416 ton, CP: 2,122 ton) (FAO, 1950 ~ 2019) (https://www.fao.org/fishery/statistics/software/fishstatj/en) (Fig. 1a). After more than 30 years since the global introduction of breeding, the main breeding areas of *S. ocellatus* were located in 11 countries and regions in the Atlantic, Pacific, Indian Oceans and Mediterranean Sea, and the total annual breeding production (taking 2019 as an example) has reached 77,008.58 tons with 1.96×10^8 USD (FAO, 1978 ~ 2019) (Fig. 1b). With more than 90 % of the total world production of *S. ocellatus* coming from China since 2003, and subsequently reaching 70,000 tons of aquaculture production starting in 2015, China has become the centre of world aquaculture production of *S. ocellatus* (www.fao.org/faostat) (Fig. 1c, d). *S. ocellatus* farming included diversified modes, such as sea cage farming, factory indoor farming, and nearshore pond farming, with sea cage farming accounting for more than 90 % of the total aquaculture production (Holt, 1993; Kang et al., 2022; Liu et al., 1998; Xue, 2008; Zhang et al., 2002). Sea cage farming was widespread along the coast of China throughout Shandong, Zhejiang, Fujian, Guangdong, Guangxi, and Hainan, and even Taiwan and Hong Kong (Kang et al., 2022; Wang and Zhang, 1998; Wang et al., 2022; Xue, 2008). Tropical cyclones have been the most influential meteorological hazard to coastal sea cage farming in China in recent decades, and as the scale of farming continues to expand, cyclone-induced waves have caused sinking and damage to cages, resulting in frequent escapes of *S. ocellatus* (Kang et al., 2022; Liang et al., 2022; Xue, 2008; Yin, 2020). Escaped *S. ocellatus* have been recorded in the western waters of Taiwan and Matsu since 1998, and frequent captures of wild *S. ocellatus* have been reported in mainland China in recent years along the coasts of Shandong, Zhejiang, Fujian, and Hainan (Liao et al., 2010; Lin et al., 2020; Wang et al., 2022; Xue, 2008). Millions of *S. ocellatus* individuals have escaped from coastal sea cages in recent years off the coast of Zhejiang and Fujian alone, and mature individuals also have been captured in natural marine areas (Kang et al., 2022; Wang et al., 2022; Xue, 2008). Recent studies have also shown that *S. ocellatus* in sea cages along the Fujian coast could spawn and fertilize naturally under suitable water temperatures (23–25 °C) and sufficient bait, which accelerated the escape of *S. ocellatus* into Chinese waters and greatly increased the possibility of population establishment (Kang et al., 2022; Wang et al., 2022; Xue, 2008). A fishery resource survey further found 28 juvenile *S. ocellatus* in subtropical mangrove habitats in the Zhujiang Estuary (Lin et al., 2020). Liao et al. (2010) reported that wild populations of *S. ocellatus* had been established in western Taiwan and the Indo-West Pacific coast as early as 2008. In recent years, there have also been fishing records of *S. ocellatus* along the offshore coasts of Korea, Singapore, and Thailand (Alidoost Salimi et al., 2021; Jaafar et al., 2012; Liao et al., 2010; Lin et al., 2020; Uyan et al., 2020; Wang et al., 2022). The escape of adults *S. ocellatus*, fertilized eggs, and juveniles into the marine ecosystem, coupled with its strong resilient biological characteristics such as fast growth rate, mixed feeding habits, disease

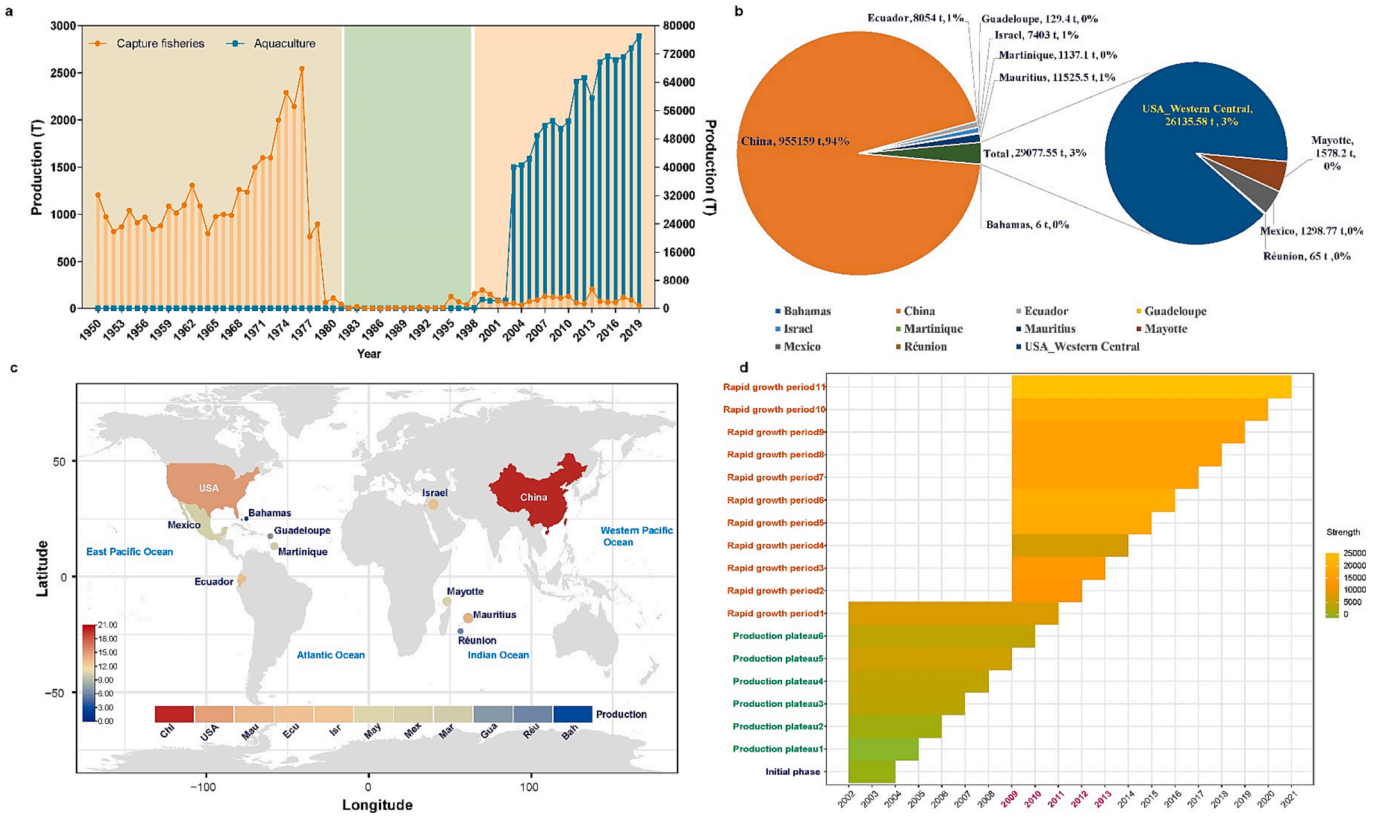

Fig. 1. Three important stages (fishing-based fisheries, 1950 ~ 1981; the nascent stage of farming, 1982 ~ 1996; rapid development of global farming, 1997 ~ 2019) in the development history of *S. ocellatus* (a) as a global fishery resource (b, c). More than 90 % of the total world production of *S. ocellatus* coming from China since 2003, and subsequently reaching 70,000 tons of aquaculture production starting in 2015 (d). Heatmap in (b) represents the total production of *S. ocellatus* in 11 major breeding countries.

resistance, high survival rate, and low oxygen tolerance, make its invasive potential very significant (Kang et al., 2022; Lin et al., 2020; Xue, 2008).

Recent studies have confirmed that the diet of escaped *S. ocellatus* has changed from feeding on chilled miscellaneous fish to main shellfish, cephalopods, small fish, and other marine organisms, which indicated its dietary composition could shift with environmental changes and has a strong ecological niche competitiveness (Jin et al., 2008; Kang et al., 2022). *S. ocellatus* was also a potentially robust carrier of diseases that would cause economic losses to the mariculture industry. Israel introduced *S. ocellatus* in 1990, with great potential for exploitation in the Mediterranean Sea and Red Sea areas, but it soon infected with Myxidiumleei (Diamant, 1998). In 2000, cultured *S. ocellatus* was also found to be infected with *Oodinium ocellatum* and *Heterophyid trematodes*, resulting in high mortality (34.6 %) in the Yunlin area of Taiwan, China (Tu et al., 2002). *S. ocellatus* has been cultured on a large scale along the southeastern coast of China, where was the main production and distribution area of other economically important fishes, such as *Nibea*, *Collichthys*, *Pennahia*, *Johnius*, and *Larimichthys crocea* (Sciaenidae) (Kang et al., 2022; Xue, 2008). Moreover, these fishes share similar ecological habits and food chain network structures with *S. ocellatus*. Currently, the practice of overfishing has resulted in a substantial depletion of wild fishery resources, including *L. crocea*, *L. polyactis*, *N. albiflora*, *J. grypotus*, and *Lateolabrax maculatus*, which occupied the top of the ecological niche, making the ecosystem incredibly fragile for them (Bai et al., 2021; Kang et al., 2022). Fishery surveys found catch rate of *L. maculatus* and Sciaenidae fishes where *S. ocellatus* could be angled and caught was extremely low (Kang et al., 2022). As an alien, large predatory fish, does *S. ocellatus* have caused a major impact on the coastal biomes and ecosystems of China, or caused a decline or even a collapse of the local endemic fishery populations? So far, almost no studies have explored this topic in China.

The present study aimed to assess the distribution and variation of *S. ocellatus* hotspot fitness zones, under global climate change, as determined by species distribution modeling (SDM), and to identify the trophic level of escaped *S. ocellatus* using stable isotope approach, and thus to provide early warning of the invasion for alien red drum *S. ocellatus* in China.

2. Materials and methods

2.1. Study system and design

In the present study, species distribution models (SDMs) were applied to statistically determine the habitat suitability of *S. ocellatus* on a global scale. Stable isotope (^{13}C, ^{15}N) techniques were used to assess the ecological status level of escaped wild *S. ocellatus* off Zhejiang Province, China (Fig. 2).

2.2. Occurrence data and assessing habitat

To obtain sufficient occurrence data, we collected georeferenced occurrence data of the whole distribution for *S. ocellatus* from the Global Biodiversity Information Facility (GBIF; https:// https://doi.org/10.15468/dl.qgxa9c), the Ocean Biogeographic Information System (OBIS; https://obis.org/) and scientific literature (Gold et al., 2001; Hollenbeck et al., 2019; Montie et al., 2016; Turner et al., 1999). A total of 25,558 records for *S. ocellatus* were acquired at the global ocean scale. A set of marine environmental variables (*e.g.*, a light at the bottom, temperature, iron concentration, salinity, dissolved oxygen concentration, *etc.*) with the corresponding current measurements were downloaded from the Bio-Oracle database at a spatial resolution of 5 arc min (9.5 km) (https://www.bio-oracle.org/) to map the potential distribution of *S. ocellatus*, as well as hotspot areas, and to identify key variables (Assis et al., 2018). In addition to the current data, future (2090 ~ 2100) marine environmental scenarios were also obtained from the Bio-Oracle database for modeling and prediction to calculate future areas of suitable habitat (Assis et al., 2018). To ensure that there was only one record per grid cell at a spatial resolution of 5 arcmins, we performed spatial filtering of all occurrences of *S. ocellatus* by trimming duplicate records using the non-metric multidimensional scaling (NMDS) method (NMTools v1.4.3, https://purl.oclc.org/enmtools), and finally retained 333 occurrences (Warren et al., 2010) (Fig. 2). All predictor variables with a raster format were changed to ASCII format using the Python-

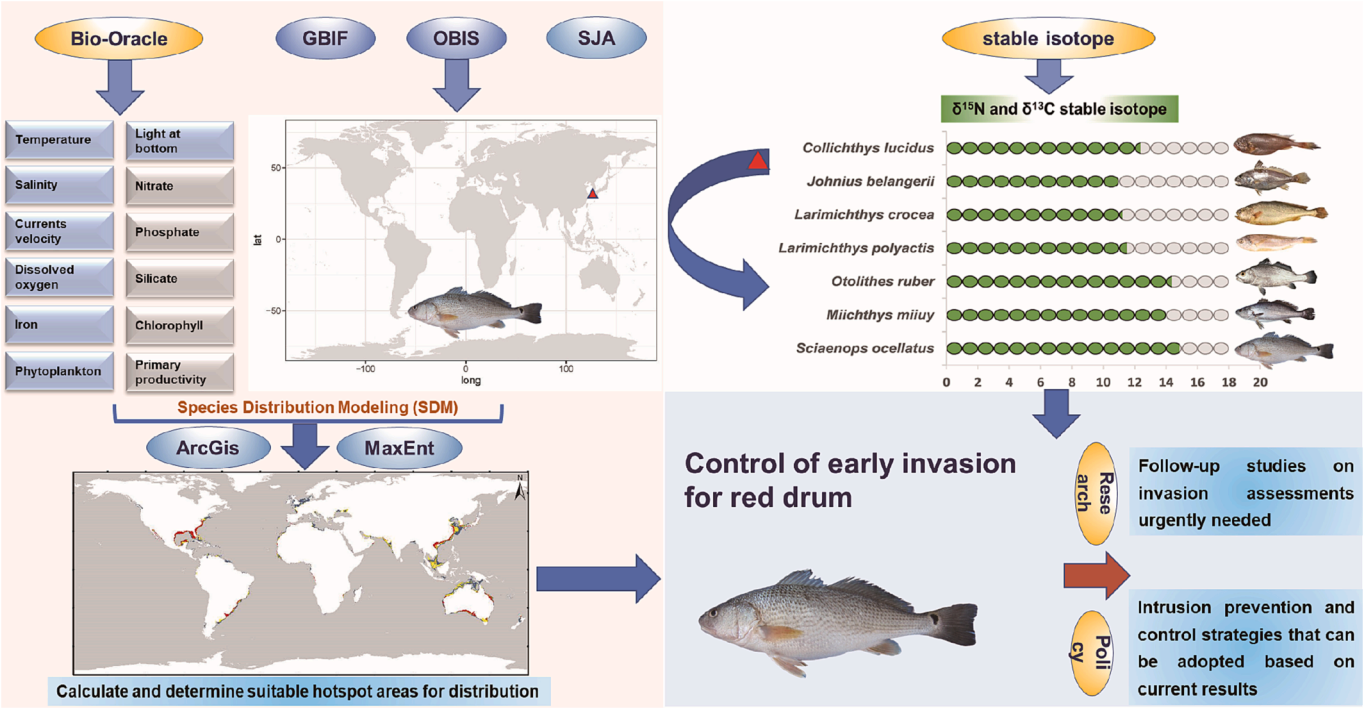

Fig. 2. Data sources for species distribution modeling, the study area of the stable isotope tracing for ecological adaptation of *S. ocellatus*.

based SDM toolbox v2.4 to perform calculations on the potential distribution areas of *S. ocellatus* with Maxent software v3.4.1 (https://www.cs.princeton.edu/~schapire/maxent/) (Brown et al., 2017; Phillips et al., 2006). To eliminate the possible negative effects of highly collinear relationships between variables, we trimmed the variables using ArcGIS v10.4 (ESRI, Redlands, CA) to calculate the relationship between sample occurrences and environmental variable data employing a Pearson correlation test for dimensionality reduction ($|r| > 0.8$) (Phillips et al., 2006) (Fig. 3a, Table S2). Seven representative marine environmental variables (temperature, salinity, phytoplankton, iron concentration, light at bottom, dissolved oxygen concentration, currents velocity in benthic layers) were retained and used for the maximum entropy model (MaxEnt v3.4.1), which has been routinely applied and has shown excellent predictive performance in various applications (Phillips et al., 2017; Phillips et al., 2006). The MaxEnt has not only been applied to successfully predict the ranges of terrestrial organisms (Melo-Merino et al., 2020), but also to successfully predict the suitable habitats of marine organisms such as *Undaria pinnatifida*, *Mytilus galloprovincialis*,

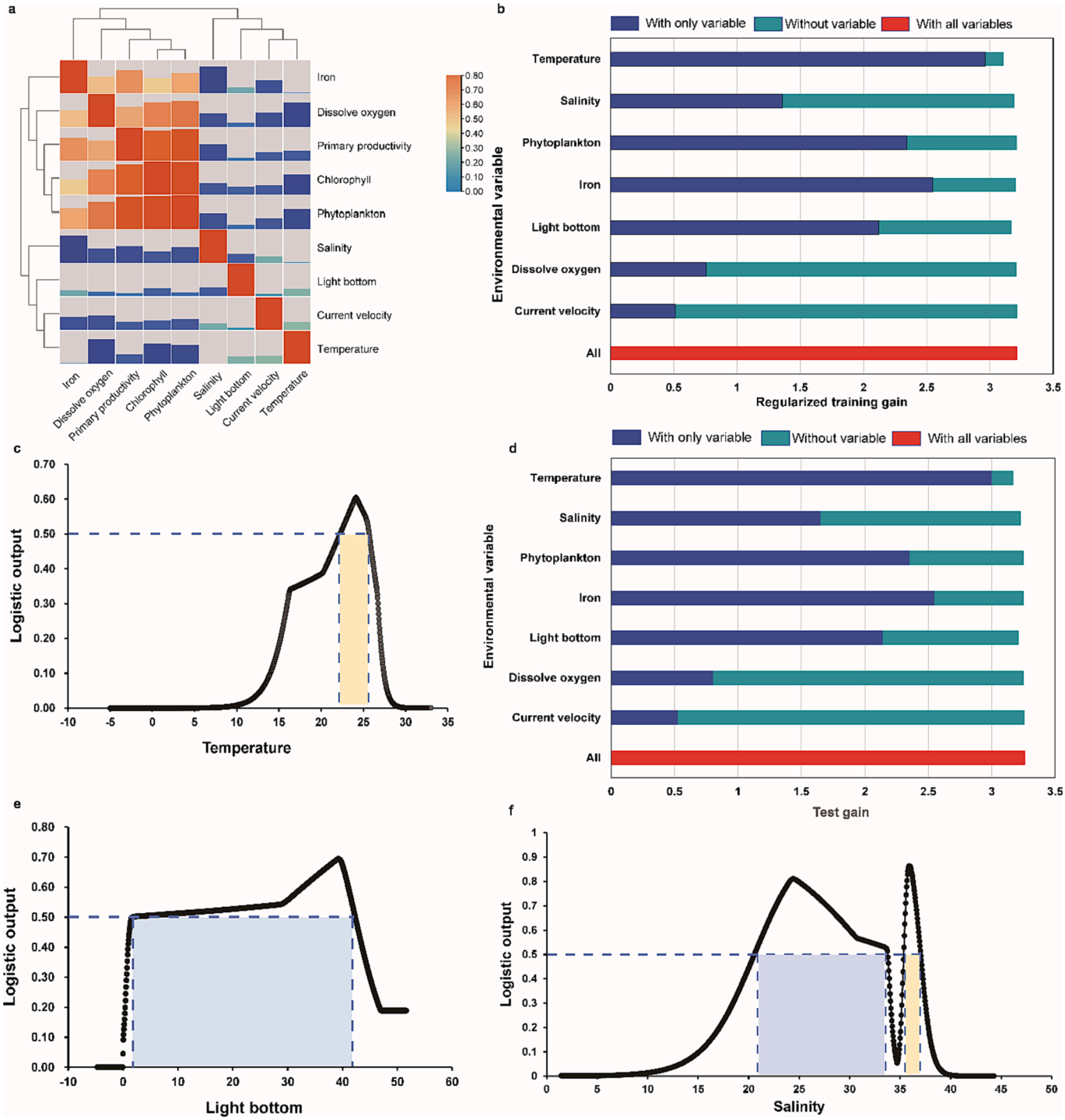

Fig. 3. Key influencing environmental variables for the distribution of *S. ocellatus* fitness zones. Relationship between sample occurrences and environmental variable data using Pearson correlation coefficient ($|r| > 0.8$) (a), the contribution of each environmental variable in the model development calculated using the jackknife test (b, d), and the response curves of key environmental variables with 10 replicate MaxEnt runs (c, e, f).

Tubastraea Tagusensis, and *Asterias amurensis*, and it has also been widely used in predicting the ranges shifts of marine fishes (Assis et al., 2015; Báez et al., 2009; Byrne et al., 2016; Carlos-Junior et al., 2015; Dulvy et al., 2008; Kleisner et al., 2017; Perry et al., 2005; Zhang et al., 2020).

Distribution suitability models for *S. ocellatus* have been developed using occurrence data and 10,000 random background points, which represented the distribution of environmental conditions in global marine areas (Phillips and Dudík, 2008). To avoid geographic bias in our model, we randomly selected 75 % of the occurrence data (both present and future) for training and fitting the model, and tested the stability of the model using the remaining 25 %. The file format was set up for logistic transformation output in a 10-fold cross-replication, which could produce output values with good visual discrimination over the entire range of values (0, lowest; 1, highest) (Phillips et al., 2017). The threshold-independent receiver operating characteristic (ROC) curve was employed to further test the performance of MaxEnt by examining the area under the ROC curve (AUC) values (>0.9) (Fig. S1) (Pearce and Ferrier, 2000; Phillips et al., 2006). We used the jackknife test to calculate the contribution of each environmental variable included in the model development (Fig. 3b, Table S3). We further calculated the value of the environmental variable with the highest training gain, which when used in isolation was considered to have the highest relative impact on the AUC of the model (Fig. 3c). MaxEnt's arithmetic results were imported into ArcGIS 10.4 for habitat suitability classification and visualization to yield the currently suitable habitat areas for *S. ocellatus* (Fig. 4a, b, Fig. S2). We then combined the MaxEnt software with the SDM Toolbox plug-in to predict future habitat suitability for *S. ocellatus* at a resolution of 5 arcmin, based on future climate scenarios for the period 2090 ~ 2100 (RCP85) (Assis et al., 2018). To evaluate the effects of climate fluctuations on suitable habitats, we converted continuous habitat suitability outputs into binary (presence/absence) maps using thresholds indicating maximum training sensitivity and specificity (Liu et al., 2013). The future areas of suitable habitat were cross-checked with the current distribution to identify areas of shifts (*e.g.*, range expansion, range contraction, no changes, *etc.*) (Fig. 4c). To further explore the dynamic migration pathways of *S. ocellatus*, we calculated the centroids of *S. ocellatus* from its current distribution to its future distribution using the Python-based SDM Toolbox (Brown et al., 2017). This analysis clustered species distributions into a single independent centroid and created a vector file describing the magnitude and direction of change over time (Hu et al., 2015). Finally, we determined the distribution shifts of *S. ocellatus* by tracking the changes of the centroids between SDMs at different time scales.

2.3. Isotope tracing for ecological adaptation

The stoichiometric composition of an organism in a given ecosystem was determined by the ingested diet. The sources of diet for species in a food web could be identified based on the principle that the stable isotopic composition of predators was close to the isotopic composition of food (Post, 2002). We used ^{13}C and ^{15}N isotope tracing techniques to characterize the food source of escaped *S. ocellatus* in the marine environment, and calculate its trophic level in the food web of the same group (Fig. 5). Fifty-eight fish (weight, 1,652 ~ 12,783 g) were caught by angling and trawling offshore the Zhejiang Province (latitude, 27°45′~28°00′; longitude, 121°15′~121°00′; surface water temperature, 19.4 ~ 29.1 ℃, bottom water temperature, 19.3 ~ 29.0℃; water depth, 12.07 ~ 20.07 m; salinity, 26.65 ~ 29.63 psu) from May 2017 to August 2018 (Fig. 5). To determine the trophic level of *S. ocellatus*, we selected catches of fish from the same batch of trawled Sciaenidae (*Miichthys miiuy*, *Otolithes ruber*, *Larimichthys polyactis*, *Larimichthys crocea*, *Johnius belangerii*, *Collichthys lucidus*) as background for isotope tracing comparison. In order to avoid any possible effects of the developmental stage on the stable isotope results, the Sciaenidae species selected for the stable isotope research mentioned above were all in the adult stage. For obtaining stable carbon and nitrogen isotope data, we collected muscle tissue (1 g) from samples of *S. ocellatus*, and other Sciaenidae species, and dried the samples in an oven (50 °C). Then, we removed 1 mg of tissue powder and placed it in a tin cup for embedding. The tin cup could be measured directly using a temperature-dependent isotope analyzer. The $^{15}N/^{14}N$ and $^{13}C/^{12}C$ ratios in the samples were detected by the analyzer (Vario Isotope cube-IsoPrime 100, Elementar, Germany). The relative amount of ^{13}C in the tissues was calculated and quantified relative to ^{12}C, expressed as $\delta^{13}C$. The $\delta^{13}C$ results were standardized and expressed relative to the Vienna Pee Dee Belemnite (VPDB), which serves as the international isotope reference scale (Liu et al., 2020). The international standard N2-atm has been used as the reference standard for the $\delta^{15}N$ (Ponton et al., 2021). $\delta^{15}N$ and $\delta^{13}C$ were calculated using the following equations: $\delta^{13}C‰ = \{((^{13}C/^{12}C \text{ sample})/(^{13}C/^{12}C \text{ PDB}))\text{-}1\}\text{the} \times 1000$, $\delta^{15}N‰ = \{((^{15}N/^{14}N \text{ sample})/(^{15}N/^{14}N \text{ atmosphere}))\text{-}1\} \times 1000$ (Bode et al., 2007; Ponton et al., 2021) (Table S4). Since the fractionation of carbon isotopes during a trophic transfer of organic matter in the food web was small (generally between 0 ~ 1 ‰), the $\delta^{13}C$ values of predators mainly reflect the characteristics of the dietary source (Post, 2002). In contrast to carbon-stable isotopes, nitrogen-stable isotopes were used to determine the trophic levels associated with different species in the food web. Research has shown that for each trophic level increased in the food web, there was a proportional increase in the $\delta^{15}N$ of the organism ranging from 2 ‰ to 4 ‰. (Peterson and Fry, 1987). Simultaneous use of multiple isotopes combined with ecological modeling could provide deeper and more complete information on the ecological fitness of species. Statistical tests for the isotope tracing comparison between *S. ocellatus* and other Sciaenidae species were performed using one-way ANOVA in GraphPad Prism software (Ferreyro et al., 2020). Dynamic heatmap histograms were generated using the OmicShare cloud statistical computing tool (https://www.omicshare.com/tools/home/report/report_histogram_heatmap.html).

3. Results

3.1. Identifying hotspot suitability regions

The AUC of *S. ocellatus* ranged from 0.981 to 0.986 (mean ± SD = 0.984 ± 0.02) on the test dataset. This result indicated that MaxEnt could be applied to accurately simulate and predict the distribution range of *S. ocellatus* at the oceanic scale under the effects of different environmental variables (Fig. S1). Three most important environmental variables influencing the distribution of *S. ocellatus* were found to be light at the bottom (54.5 %), temperature (37.6 %), and iron concentration (primary productivity) (4.8 %) based on the jackknife method calculation, with a total cumulative contribution of 96.9 % to the MaxEnt model (Fig. 3b, Table S3). Four categories (non-suitable habitats, 0 ~ 0.2; low-adaptive areas, 0.2 ~ 0.4 with 3,350,699 km^2; moderate growth areas, 0.4 ~ 0.6 with 1,682,359 km^2; highly suitable areas, 0.6 ~ 1 with 1,248,974 km^2) was designed with threshold of 0.20 by using the sensitivity–specificity sum maximization approach (Fig. 4a). Four hot-spot suitable regions for *S. ocellatus* were first identified on a global scale in the Atlantic Ocean along the Gulf of Mexico, and the Uruguayan coasts, and in the Pacific Ocean along the Chinese and Australian coasts (Fig. 4a). Notably, while the suitable range of *S. ocellatus* showed a discontinuous distribution layout over the world's oceans, there was a strong continuous distribution pattern of regional suitable areas existed, especially along the Gulf Coast in the western Atlantic Ocean and the coasts of China and Australia in the western Pacific Ocean (Fig. 4). There was also a substantial amount of moderately suitable areas for *S. ocellatus* in nearshore areas, such as the Arabian Sea coast in the Indian Ocean, Morocco, Mauritania and Senegal in the eastern Atlantic Ocean, which have no records of *S. ocellatus* culture production (Fig. 4, Fig. S2).

Recent projection models suggested that suitable habitats would experience expansion events in the near future (Fig. 4c). Under the

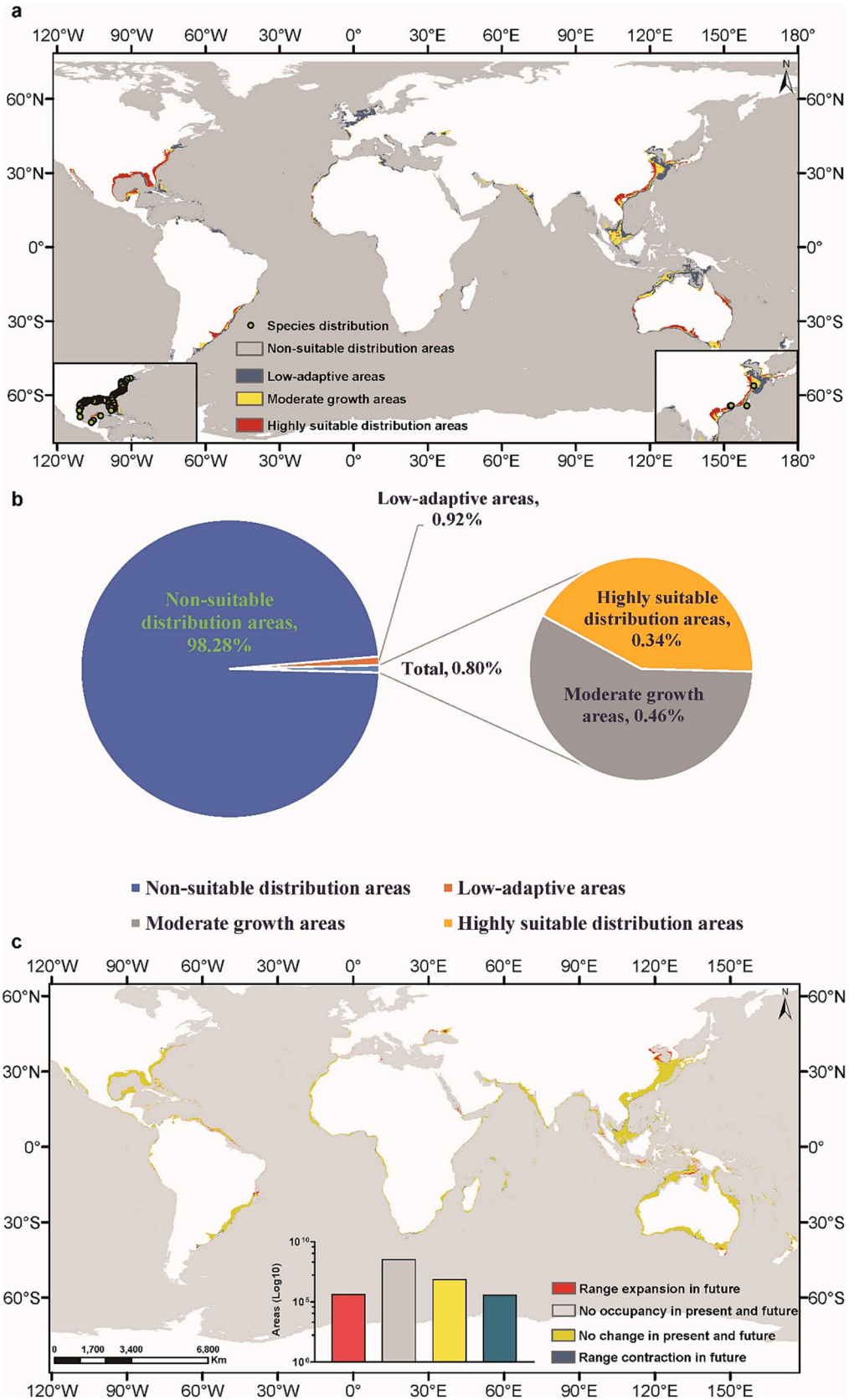

Fig. 4. Identified distribution hotspot fitness zones of *S. ocellatus* according to current environmental conditions (a, b) and forecasted shifts of the habitat distribution center in future climate scenarios (RCP8.5). Highly suitable areas (0.6 ~ 1) with 1,248,974 km^2 were designed with the threshold of 0.20 by using the sensitivity–specificity sum maximization approach (a, b), and suitable habitat will expand moderately by 448,178 km^2 from the present to the 2090 ~ 2100 period under the current potential distribution range (c). The left and right panels of figure (a) showed the distribution of sample records from the Gulf of Mexico and China coast, respectively.

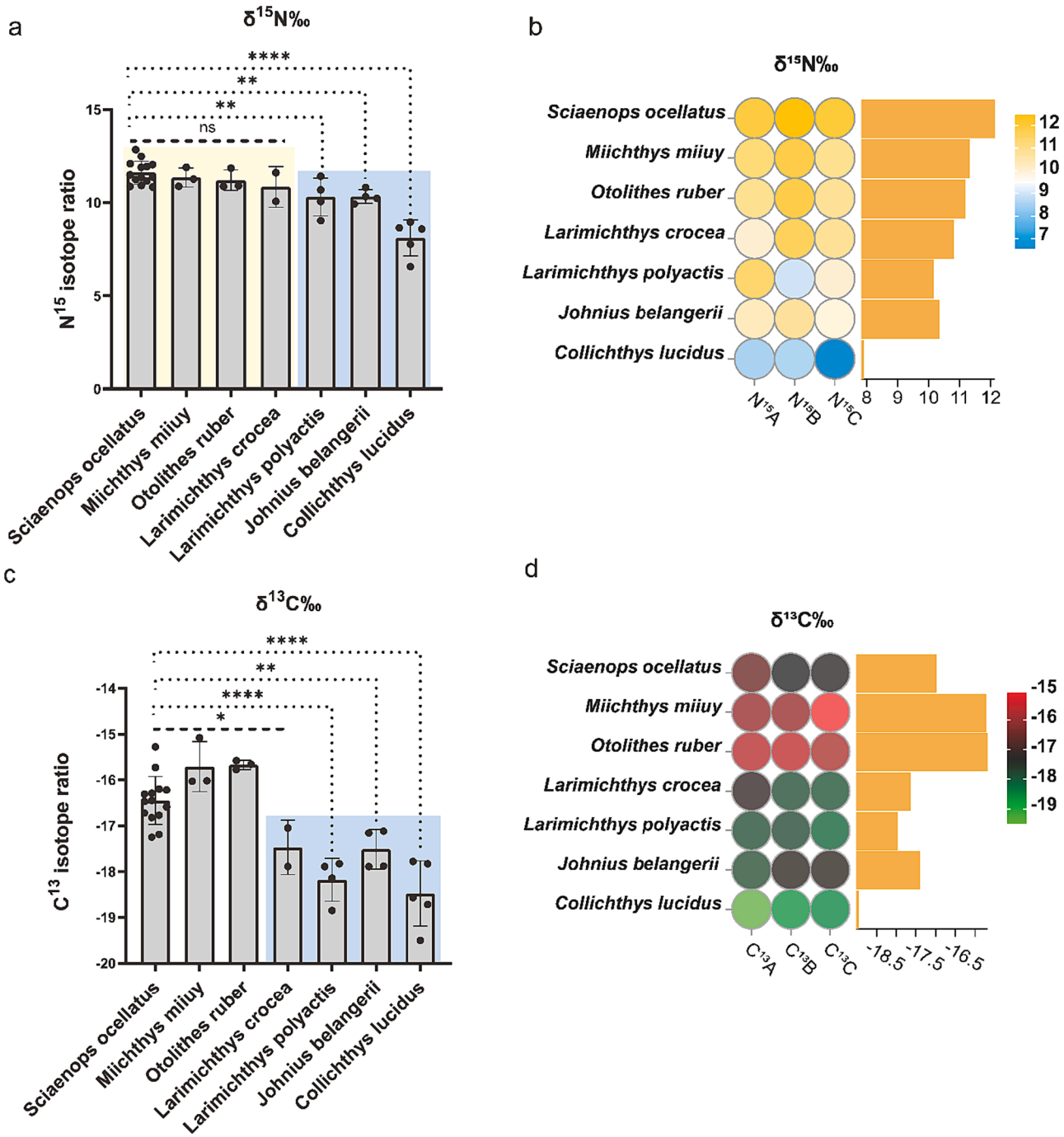

Fig. 5. Determined the trophic level in the food web of escaped *S. ocellatus* offshore the Zhejiang Province (China) using $\delta^{15}N$ (a, b) and $\delta^{13}C$ (c, d) with the Sciaenidae fish in the identical waters as background for isotope tracing comparison. Species involved in the comparison: *M. miiuy*, *O. ruber*, *L. polyactis*, *L. crocea*, *J. belangerii*, *C. lucidus*; Significance: ns > 0.05, *p < 0.05, **p < 0.01, ***p < 0.001, ****p < 0.0001.

RCP8.5 scenarios, suitable habitat for *S. ocellatus* may expand moderately by 448,178 km^2 from the present to the 2090 ~ 2100 period under the current potential distribution range. Notably, suitable habitats for the northwards (448,178 km^2) of *S. ocellatus* were concentrated in the northern Black Sea, the Gulf of Aden in the Red Sea, the coast of Bahia State in Brazil, the northern Yellow Sea and Bohai Sea coast of China, and the Arafura Sea off the north coast of Australia (Fig. 4c, Fig. S3). The centre of the current distribution of *S. ocellatus* was identified by centroid migration analysis to be located at 56.57 E and 3.73 N, derived from the global habitat discontinuity and potential wide-range habitat for *S. ocellatus* in the western Pacific (Fig. 4c). The future potential centroid would shift to the northwest (57.64 E, 4.13 N) under the future emission scenario (RCP8.5), which was far from the present potential centroid by up to 115.28 km.

3.2. Isotope tracing reveals ecological competitiveness

To prevent stable isotope ratio variations that could arise from different types of bait species and their abundance in different areas of the sea, we selected the same batch of surveyed catch species for stable isotope tracing studies. Our stable isotope results showed that the range of $\delta^{15}N$ in the main fishery organisms (Sciaenidae) within the occurrence area of *S. ocellatus* in the East China Sea was from 6.57 ‰ to 12.84 ‰, and the average value was 10.71 ‰, with a total span of 6.27 ‰

(Fig. 5ab). One-way ANOVA revealed significant differences ($p < 0.05$) in $\delta^{15}N$ among Sciaenidae species in the present study, and multiple comparison analysis showed that there were significant variations ($p < 0.05 \sim 0.001$) in $\delta^{15}N$ between *S. ocellatus* (10.84 ~ 12.84 ‰, 11.61 ± 0.62 ‰) and miniaturized species within Sciaenidae (*L. polyactis* 9.03 ~ 11.42 ‰, 10.30 ± 1.01 ‰, *J. belangerii* 9.93 ~ 10.82 ‰, 10.33 ± 0.37 ‰, *C. lucidus* 6.57 ~ 8.96 ‰, 8.11 ± 0.97 ‰) with a total span from 1.28 ‰ to 3.50 ‰ (Fig. 5ab). The stable *N* isotope ratio ($\delta^{15}N$) results further showed non-significant differences ($p > 0.05$) between *S. ocellatus* and large benthic predatory fish in Sciaenidae (*M. miiuy* 10.88 ~ 11.90 ‰, 11.35 ± 0.51 ‰; *O. ruber* 10.87 ~ 11.85 ‰, 11.21 ± 0.56 ‰; *L. crocea* 10.07 ~ 11.61 ‰, 10.84 ± 1.09 ‰) with a total span from 0.26 ‰ to 0.77 ‰ (Fig. 5a, b). Stable *N* isotope ratio results further showed that the $\delta^{15}N$ values of *S. ocellatus* were slightly but non-significantly higher than those of the large benthic predatory fish in Sciaenidae (*M. miiuy* 11.35 ± 0.51 ‰; *O. ruber* 11.21 ± 0.56 ‰; *L. crocea* 10.84 ± 1.09 ‰) differences ($p > 0.05$) with a total span of 0.26 ‰ to 0.77 ‰ (Fig. 5a, b, Table S4). Our results showed that miniaturized fish species tended to have lower $\delta^{15}N$ values as predators and that with increasing size of the predator species, the $\delta^{15}N$ values increased, as reported in many previous studies (Fig. 5a, b) (Bai et al., 2021; Layman et al., 2007; Yan et al., 2012). This study thus confirmed that escaped *S. ocellatus* possessing high $\delta^{15}N$ values has similar ecological niche competitiveness to other large predatory fishes in the East China Sea.

Our results based on a multidimensional statistical analysis of $\delta^{13}C$ showed extremely significant differences ($p < 0.0001$) between *S. ocellatus* (-15.28 ~ -17.25 ‰, −16.45 ± 0.52 ‰) and miniaturized species within Sciaenidae (*L. polyactis* −17.83 ~ -18.85 ‰, −18.18 ± 0.47 ‰; *J. belangerii* −17.12 ~ -17.89 ‰, −17.51 ± 0.43 ‰; *C. lucidus* −17.78 ~ -19.50 ‰, −18.48 ± 0.71 ‰) with a span from 1.06 ‰ to 2.03 ‰, while showing a slightly significant level of difference ($p < 0.05$) compared to large benthic predatory fish (*M. miiuy* −15.08 ~ -16.03 ‰, −15.71 ± 0.54 ‰; *O. ruber* −15.58 ~ -15.78 ‰, −15.68 ± 0.10 ‰; *L. crocea* −17.05 ~ -17.89 ‰, −17.47 ± 0.59 ‰) with a span from 0.73 ‰ to 1.02 ‰ (Fig. 5c, d, Table S4). The results of the present study showed that the $\delta^{13}C$ of *S. ocellatus* was similar to that of $\delta^{15}N$, and its food composition and sources were very similar to those of large benthic fishes such as *M. miiuy*, *O. ruber* and *L. crocea*. Our results further revealed that *S. ocellatus* could directly prey on *J. belangerii* from a dominant ecological position compared to benthic small fishes such as *L. polyactis*, *J. belangerii*, and *C. lucidus* (Fig. 5c, d, Table S4).

4. Discussion

This study integrated SDMs and stable isotope tracing approaches to identify potentially suitable habitat zones of *S. ocellatus* and shifts in habitat zones under climate change. The trophic level of escaped *S. ocellatus* was also explicitly estimated. Our results showed that the coastal waters of China and Australia in the western Pacific Ocean, in addition to the Gulf of Mexico, were excellent long-term habitats for *S. ocellatus*. Here, we confirmed that escaped *S. ocellatus* was dominant from the perspective of feeding sources and food webs under wild conditions offshore China. In our study, we combined macroscopic and microscopic approaches to recognize that global artificial introgression breeding had broken the discontinuous pattern for *S. ocellatus* submerged in suitable habitats at the oceanic scale, and its unique biological characteristics (*e.g.*, fast growth rate, mixed food habits, strong reproductive ability, disease resistance, low oxygen tolerance, *etc.*) had enabled it to rapidly adapt and occupy new ecological niches in potential new suitable areas. Our study confirmed *S. ocellatus* had extremely strong invasive potential, which allowed this fish to have already established a competitive situation with indigenous species from the perspective of potential habitat prediction calculations, and ecological niches of wild samples.

4.1. Environment-driven potential habitat formation and shifts

Species distribution models (SDMs), based on the maximum entropy method (MaxEnt), have a good predictive performance to identify the effects of climate change on terrestrial and freshwater species habitat suitability (Phillips et al., 2017; Phillips et al., 2006; Phillips and Dudík, 2008; Robinson et al., 2011; Robinson et al., 2017; Zhang et al., 2020). Our model predictions suggested the Gulf Coast was a suitable hotspot for *S. ocellatus*, corresponding to the present-day distribution pattern of *S. ocellatus* fishery resource investigations (Ackerly et al., 2022; Bacheler et al., 2012; Craig et al., 1995; Forsberg et al., 1996; Watson et al., 2014). In addition, three other potential hotspots were also predicted for *S. ocellatus* by our model, located along the Uruguayan coast in the Atlantic Ocean and on the Chinese and Australian coasts in the Pacific Ocean (Fig. 4a). Records of sea cage farming in 11 countries and regions around the world (*e.g.*, Bahamas, China, Ecuador, Guadeloupe, Israel, Mexico, *etc.*), together with the survey of wild fishery resources for escaped *S. ocellatus*, demonstrated that this fish had several discontinuous potential suitable habitats around the world consistent with our model predictions (Fig. 1, Fig. 4) (FAO). According to our model, the temperature was one of the most important factors (*regularized training gain* = 2.96/3.11, *test gain* = 2.99/3.17) regulating the distribution of *S. ocellatus*. Such temperature-driven habitat location determination has been previously reported for many species (*e.g.*, *Gadus morhua*, *Solea solea*, *Arnoglossus laterna*, *Lumpenus lampretaeformis*, *Hippoglossoides platessoides*, *etc.*) (Dulvy et al., 2008; Fossheim et al., 2015; Perry et al., 2005; Sandø et al., 2020; Zhang et al., 2020). We further revealed that light at the bottom (1.73 ~ 40.36, *logistic output* ≥ 0.5) was another important environmental factor modulating the potentially suitable habitat for *S. ocellatus*, with a contribution rate of 54.5 % to our predicted SDM model (Table S1, Fig. 3). Low light at bottom levels (*LB* < 65) often occurred in the estuaries of rivers rich in nutrients and phytoplankton, such as the Mississippi River estuary in the Gulf of Mexico, the Negro River estuary in Uruguay, the Yangtze and Pearl River estuaries in China, and the Yarra River and Victoria River estuary in Australia, which were consistent with the ecological habits of *S. ocellatus* (Bui et al., 2013; Chen and Zhao, 2021; Dahms et al., 2017; Douglas, 2018; Langbehn and Varpe, 2017; Picapedra et al., 2018; Watson et al., 2014).

Under the present SDM evaluation, projections also suggested that future climate change would likely lead to a global expansion in suitable habitats for *S. ocellatus*, with a northwards shift in the suitable habitat centroid (Fig. 4). Such climate-induced shifts in habitat have been previously reported for many marine species (Cheung et al., 2013; Dulvy et al., 2008; Kleisner et al., 2017; Perry et al., 2005; Potts et al., 2014; Sandø et al., 2020; Zhang et al., 2020). Perry et al. (2005) identified a northwards shift in the distribution centres for 15 species of demersal fish (*e.g.*, *Gadus morhua*, *Solea solea*, *Trisopterus luscus*, *etc.*) on the North Sea coast in response to climate warming. Sandø et al. (2020) found that future climate-driven (RCP4.5) changes in temperature and salinity caused the spawning grounds of the Northeast Arctic cod to shift northeastward. It was notable that the near-future expansion in suitable habitats (448,178 km^2) for *S. ocellatus* would occur mainly in the northern Yellow Sea of China and throughout the Bohai Sea in the Pacific Ocean and in the northern nearshore waters of Australia, which were spawning and hatching areas for the major fishery species in offshore China and the centre of marine fish biodiversity in the Indo-Pacific convergence zone, respectively (Fig. 4c) (Chen and Huang, 2021; Fang et al., 2011; Liu and Xiao, 2021; Xu, 2021). Considering the globalization of aquaculture of introduced *S. ocellatus*, the discontinuous distribution of potentially suitable regions at the global scale together with the continuous distribution pattern of wide suitable habitats within the region provided the necessary ecological and introductory conditions for *S. ocellatus* to enter new suitable regions in addition to the Gulf of Mexico (Fig. 4a). Using eDNA methods, Wang et al. (2022) detected a high abundance (61.36 %) of *S. ocellatus* in the Jiaojiang Estuary and Sanmen Bay area with low light at bottom levels in the East China Sea,

which was consistent with the predictions of our SDM (Fig. 3). Considering the dominant biological properties of *S. ocellatus* and the existence of a wide range of suitable habitats worldwide, we must pay close attention to whether *S. ocellatus* will become another worldwide invasive species after *Lutjanus kasmira* and *Pterois volitans/miles* (Bogdanoff et al., 2018; Hixon et al., 2016; Peake et al., 2018; Sancho et al., 2018).

4.2. Eco-competitiveness driving habitat expansion and colonization

Due to layer-by-layer enrichment characteristics of ^{15}N in the food chain, $\delta^{15}N$ has been demonstrated to strongly determine the trophic level of organisms, with an average threshold of 3.4 ‰ across trophic levels (Minagawa and Wada, 1984; Miyake and Wada, 1967; Post, 2002). Our results revealed that escaped *S. ocellatus* in Chinese waters showed the highest $\delta^{15}N$ values (11.61 ± 0.62 ‰) compared with those of typical fishery fish in the same waters, and the difference ranged from 0.26 ‰ to 3.5 ‰, spanning at least two trophic levels (Fig. 5ab). Typical fishery fish, which were at high trophic levels due to their aggressive predatory ability with large $\delta^{15}N$ values, were mostly reported offshore of China, such as *Trichiurus lepturus* (11.6 ± 0.9 ‰), *Lophius litulon* (11.8 ± 1.4 ‰), *Argyrosomus argentatus* (11.8 ± 0.7 ‰), *Anago anago* (11.3 ± 0.1 ‰) and *Psenopsis anomala* (11.8 ± 0.7 ‰) (Ji et al., 2011; Yan et al., 2012). Similar cases of magnified fish with larger $\delta^{15}N$ values have been reported for fish communities in the Atlantic Celtic Sea and the North Sea (Jennings et al., 2002). Fish always have a wide range of food habits and could feed on plankton, crustaceans, and small fish, and their food habits change during different growth periods, so the $\delta^{15}N$ of fish was typically high. Where the $\delta^{15}N$ of some different groups of organisms overlapped, this was often associated with them preying on the same bait species, suggesting that interspecific competition was occurring (Qin et al., 2020; Wang et al., 2021). Our stable ^{15}N isotope tracing results also confirmed that escaped *S. ocellatus* (11.61 ± 0.62 ‰) showed a significant change in feeding habits and occupied the same trophic level as the dominant indigenous fish species (*e.g.*, *M. miiuy*, *O. ruber*, *L. crocea*, *Trichiurus lepturus*, *Lophius litulon*, *A. argentatus*, *etc.*) in the East China Sea, showing extremely significant overlap of ecological niches with strong ecological competitiveness (Fig. 5a, b) (Ji et al., 2011; Lin et al., 2020; Xue, 2008).

Previous studies have reported that $\delta^{13}C$ enrichment in the same trophic level was usually less than 1.0 ‰ and increased with the deepening of the biogenic water layer, which could be used as an indicator of biogenic habitat or carbon source (Davenport and Bax, 2002; Vander Zanden and Vadeboncoeur, 2002). The $\delta^{13}C$ results in this study showed that *S. ocellatus* (-16.45 ± 0. 52 ‰) shared comparable biological habitats and food carbon sources (0.73 ~ 1.02 ‰) with representative macrobenthic predatory fishes within Sciaenidae in the East China Sea, and this was consistent with the $\delta^{15}N$ results (Fig. 5). The range overlap of $\delta^{13}C$ between *S. ocellatus* and other large predatory fishes indicated that their food sources were cross-mixed, further suggesting that *S. ocellatus* formed overlapping and competing ecological niches with dominant native fish species in escaped waters (Fig. 5). Our study was further confirmed by previously reported fishery surveys on the stomach contents of escaped *S. ocellatus* in the East China Sea, involving bait taxa of at least 49 species in six major groups (20 species of fish, 13 species of short-tailed, 11 species of long-tailed, 3 species of cephalopods, and 1 species each of stomatopods and polychaetes) (Xue, 2008). In addition, it was suggested that in the same ecosystem, if the carbon stable isotope difference between two species was more than 0.60 ‰ and less than 1.5 ‰, a predation relationship between these two species was considered (Bai et al., 2021). Our findings indicated *S. ocellatus* could directly predate (0.60 ~ 1.5 ‰) *M. miiuy*, *O. ruber* and *L. crocea* at the same trophic level with $\delta^{13}C$ ranging from 0.73 ‰ to 1.02 ‰, demonstrating that *S. ocellatus* has extremely competitive ecological niches in the escape waters (Fig. 5). Although the $\delta^{13}C$ span among *S. ocellatus, L. polyactis* and *C. lucidus* ranged from 1.73 ‰ to 2.03 ‰, thus over 1.5 ‰, and they might be at different trophic levels, the significant predatory relationship between *S. ocellatus* and these two species was confirmed by our $\delta^{13}C$ values and the stomach content results (Fig. 5) (Xue, 2008).

The present study quantifies and confirms for the first time where *S. ocellatus* was located at the top of the food web in the escape zone in terms of $\delta^{13}C$ and $\delta^{15}N$. As we mentioned above, the global introduction of artificial aquaculture has provided the necessary conditions for the expansion of *S. ocellatus* populations in potentially suitable habitats on a global scale, and highly competitive ecological niches have provided excellent ecological conditions for the rapid population colonization of *S. ocellatus*. Therefore, the global scale continuous habitat area of *S. ocellatus* coupled with its strong ecological niche competitiveness would certainly draw our attention and warning.

4.3. Control of early invasion for red drum

According to our multidisciplinary procedure using SDMs, and stable isotope tracking approaches for scientific risk assessment of early invasion, we found that *S. ocellatus* had established a competitive situation with native species and entered the process of invasive colonization and latency period in the escape zone of coastal China (Fig. 4, Fig. 5, Fig. 6). Recent reports on eDNA and fisheries resources also confirmed the presence of wild populations of *S. ocellatus* in the offshore waters of the Yangtze River and Pearl River Estuary in China (Kang et al., 2022; Wang et al., 2022). Notably, there has been an increasing number of reports of *S. ocellatus* being caught in hotspot habitat areas in recent years, such as Singapore, Thailand, Taiwan Strait of China, East China Sea, South China Sea, South Korea, and other coastal waters (Alidoost Salimi et al., 2021; Jaafar et al., 2012; Liao et al., 2010; Uyan et al., 2020; Wang et al., 2022). Therefore, the global scale continuous habitat area of *S. ocellatus* coupled with its strong ecological niche competitiveness would certainly draw our attention and warning and implement effective actions to control the invasion.

First, it is necessary to reduce the number of escaped *S. ocellatus* into the sea from the origin, including adults and spawning juveniles, to cut off the continuous supplementation of breeding resources for the escaped population of *S. ocellatus* in the waters of the suitable area, and to prevent *S. ocellatus* from forming natural spawning and reproduction populations in the escaped waters. Second, multidisciplinary procedures (*e.g.,* fishery surveys of eggs and juveniles, migration tracking, *etc.*) and advanced techniques (*e.g.,* DNA barcoding, otolith isotopes, *etc.*) are needed for further use to scientifically assess the invasion stage (*e.g.,* colonization period, dispersal period, outbreak period, *etc.*) of *S. ocellatus*. At the same time, with the expansion of aquaculture, there is a need for a special administrative function to formulate a clear policy on the introduction of non-native species (INN) and to use it as a basis for the formulation of culture and breeding patterns for the INN species (*eg.* factory farming, marine cages farming, and pond farming, *etc.*). At present, the breeding mode of *S. ocellatus* is mainly inshore cages and pond culture, which can escape from high-density culture ponds in low-lying areas or marine cages during floods (Kang et al., 2022; Liao et al., 2010; Wang et al., 2022). Policy-driven changes in *S. ocellatus* culture patterns (switching from sea-cage culture to land-based culture ponds and factory farming) are the most effective tools available to cut off the invasive spread of *S. ocellatus* in the escape zone of coastal China. Third, it is necessary to increase the publicity on the devastating impact of invasive species on biodiversity, to raise people's alertness to the use of INN species resources, and especially to strictly prohibit the stocking and release of INN species in native waters.

5. Conclusions

The unprecedented frequency of *S. ocellatus* escapes from sea cages (million tail level) in recent decades has put enormous pressure on local marine biodiversity and ecosystems. Our study first identified four hotspot fitness zones for *S. ocellatus* at the global scale located in the Atlantic Ocean along the Gulf of Mexico and Uruguayan coasts, and in

the Pacific Ocean along the Chinese and Australian coasts based on the species distribution model analyses. Under global warming and climate change, the most suitable habitat for *S. ocellatus* would be expanded (448,178.6 km^2) and the centre of mass would shift northwards. Stable isotope $\delta^{15}N$ and $\delta^{13}C$ ratios showed that *S. ocellatus* had very high ecological competition with a wide feeding range and high ecological position in the escape zone off the coast of China. Our study confirmed *S. ocellatus* had extremely strong invasive potential and has already established a competitive situation with indigenous fauna from the perspective of potential habitat prediction calculations, ecological niches of wild samples. Since our study did not involve a monitoring experiment of *S. ocellatus* eggs and juveniles, there was an urgent need for a follow-up study to monitor *S. ocellatus* egg and juvenile fishery resources in the hotspot habitat to determine their content and spatial density variation in real-time and to provide additional information on wild germplasm resources for the invasion and prevention and control of *S. ocellatus*.

CRediT authorship contribution statement

Yongshuang Xiao: Conceptualization, Formal analysis, Methodology, Software, Validation, Visualization, Writing – original draft, Writing – review & editing, Funding acquisition. **Jing Liu:** Conceptualization, Formal analysis, Methodology, Supervision, Validation, Visualization, Writing – original draft, Writing – review & editing, Funding acquisition. **Jiehong Wei:** Data curation, Validation, Visualization, Writing – original draft. **Zhizhong Xiao:** Validation, Visualization, Writing – original draft. **Jun Li:** Data curation, Validation, Visualization, Writing – original draft. **Alfonso Aguilar-Perera:** Data curation, Validation, Visualization, Writing – review & editing. **Angel Herrera-Ulloa:** Data curation, Validation, Visualization, Data curation, Writing – review & editing.

Declaration of Competing Interest

The authors declare that they have no known competing financial interests or personal relationships that could have appeared to influence the work reported in this paper.

Data availability

Data will be made available on request.

Acknowledgments

This work was supported by the Strategic Priority Research Program of the Chinese Academy of Sciences (No. XDB42000000), National Natural Science Foundation of China (No. 42276107; No. 32270472); Biodiversity Conservation Strategy, CAS Strategic Biological Resources Service Network Program (ZSSD-019), Key Deployment Project of Center for Ocean Mega-Science, Chinese Academy of Sciences (COMS2020Q05), National Key Research and Development Program (2022YFC3103600). We thank Mr. Kaida Xu (Zhejiang Marine Fisheries Research Institute, Zhejiang, China) for their help with wild fish sample collection and hydrological data acquisition. We thank anonymous reviewers for their helpful comments and suggestions.

Appendix A. Supplementary data

Supplementary data to this article can be found online at https://doi.org/10.1016/j.ecolind.2023.111069.

References

Ackerly, K.L., Roark, K.J., Nielsen, K.M., 2022. Short-term Salinity Stress During Early Development Impacts the Growth and Survival of Red Drum (Sciaenops ocellatus). Estuar. Coasts.

Alidoost Salimi, P., Creed, J.C., Esch, M.M., Fenner, D., Jaafar, Z., Levesque, J.C., Montgomery, A.D., Alidoost Salimi, M., Edward, J.K.P., Raj, K.D., Sweet, M., 2021. A review of the diversity and impact of invasive non-native species in tropical marine ecosystems. Mar. Biodivers. Rec. 14, 11.

Assis, J., Tyberghein, L., Bosch, S., Verbruggen, H., Serrão, E.A., De Clerck, O., 2018. Bio-ORACLE v2.0: Extending marine data layers for bioclimatic modelling. 27, 277-284.

Assis, J., Zupan, M., Nicastro, K.R., Zardi, G.I., McQuaid, C.D., Serrao, E.A., 2015. Oceanographic Conditions Limit the Spread of a Marine Invader along Southern African Shores. PLoS One 10, e0128124.

Bacheler, N.M., Buckel, J.A., Paramore, L.M., 2012. Density-dependent habitat use and growth of an estuarine fish. Can. J. Fish. Aquat. Sci. 69, 1734–1747.

Báez, J.C., Olivero, J., Peteiro, C., Ferri-Yáñez, F., Garcia-Soto, C., Real, R., 2009. Macro-environmental modelling of the current distribution of Undaria pinnatifida (Laminariales, Ochrophyta) in northern Iberia. Biol. Invasions 12, 2131–2139.

Bai, H.Y., Wang, Y.K., Zhang, T.T., Huang, L.F., Sun, Y., 2021. Trophic Levels and Feeding Characters of Marine Fishes in the Yellow Sea and Northern East China Sea Based on Stable Isotope Analysis. Progr. Fish. Sci. 42, 10–17.

Bailey, S.A., 2015. An overview of thirty years of research on ballast water as a vector for aquatic invasive species to freshwater and marine environments. Aquat. Ecosyst. Health Manag. 18, 261–268.

Blossey, B., 1999. Before, During and After: The Need for Long-term Monitoring in Invasive Plant Species Management. Biol. Invasions 1, 301–311.

Bode, A., Alvarez-Ossorio, M.T., Cunha, M.E., Garrido, S., Peleteiro, J.B., Porteiro, C., Valdés, L., Varela, M., 2007. Stable nitrogen isotope studies of the pelagic food web on the Atlantic shelf of the Iberian Peninsula. Prog. Oceanogr. 74, 115–131.

Bogdanoff, A.K., Mostowy, J., Peake, J., Layman, C.A., Bermudez, A.B., Baca, C.G., Palacios, N.H., Gonzalez, D.T.M., Del Rocio Bravo Xicoténcatl, M., Morris, J.A., 2018. A brief description of invasive lionfish (Pterois sp.) diet composition in the Arrecifes de Cozumel National Park. Food Webs 17, e00104.

Breitwisch, R., 2001. Alien Species in North America and Hawaii: Impacts on Natural Ecosystems. The Auk 118.

Brown, J.L., Bennett, J.R., French, C.M., 2017. SDMtoolbox 2.0: the next generation Python-based GIS toolkit for landscape genetic, biogeographic and species distribution model analyses. PeerJ 5, e4095.

Bui, S., Oppedal, F., Korsøen Ø, J., Sonny, D., Dempster, T., 2013. Group behavioural responses of Atlantic salmon (Salmo salar L.) to light, infrasound and sound stimuli. PLoS One 8, e63696.

Byrne, M., Gall, M., Wolfe, K., Aguera, A., 2016. From pole to pole: the potential for the Arctic seastar Asterias amurensis to invade a warming Southern Ocean. Glob. Chang. Biol. 22, 3874–3887.

Carlos-Junior, L.A., Neves, D.M., Barbosa, N.P., Moulton, T.P., Creed, J.C., 2015. Occurrence of an invasive coral in the southwest Atlantic and comparison with a congener suggest potential niche expansion. Ecol. Evol. 5, 2162–2171.

Chen, N.S., Huang, H.L., 2021. Advances in the study of biodiversity of phytoplankton and red tide species in china (i): the Bohai sea. Oceanologia Et Limnologia Sinica 52, 346–362.

Chen, Y., Zhao, H., 2021. Spatial distribution of the summer subsurface chlorophyll maximum in the North South China Sea. PLoS One 16, e0248715.

Cheung, W.W., Watson, R., Pauly, D., 2013. Signature of ocean warming in global fisheries catch. Nature 497, 365–368.

Cowie, R.H., 1998. Patterns of introduction of non-indigenous non-marine snails and slugs in the Hawaiian Islands. Biodivers. Conserv. 7, 349–368.

Craig, S.R., Neill, W.H., Gatlin, D.M., 1995. Effects of dietary lipid and environmental salinity on growth, body composition, and cold tolerance of juvenile red drum (Sciaenops ocellatus). Fish Physiol. Biochem. 14, 49–61.

Cuthbert, R.N., Pattison, Z., Taylor, N.G., Verbrugge, L., Diagne, C., Ahmed, D.A., Leroy, B., Angulo, E., Briski, E., Capinha, C., Catford, J.A., Dalu, T., Essl, F., Gozlan, R.E., Haubrock, P.J., Kourantidou, M., Kramer, A.M., Renault, D., Wasserman, R.J., Courchamp, F., 2021. Global economic costs of aquatic invasive alien species. Sci. Total Environ. 775, 145238.

Dahms, H.U., Tseng, L.C., Hwang, J.S., 2017. Are vent crab behavioral preferences adaptations for habitat choice? PLoS One 12, e0182649.

Davenport, S.R., Bax, N.J., 2002. A trophic study of a marine ecosystem off southeastern Australia using stable isotopes of carbon and nitrogen. Can. J. Fish. Aquat. Sci. 59, 514–530.

Diamant, A., 1998. Red drum Sciaenops ocellatus (Sciaenidae), a recent introduction to Mediterranean mariculture, is susceptible to Myxidium leei (Myxosporea). Aquaculture 162, 33–39.

Douglas, R.H., 2018. The pupillary light responses of animals; a review of their distribution, dynamics, mechanisms and functions. Prog. Retin. Eye Res. 66, 17–48.

Dukes, J.S., Mooney, H.A., 1999. Does global change increase the success of biological invaders? Trends Ecol. Evol. 14, 135–139.

Dulvy, N.K., Rogers, S.I., Jennings, S., Stelzenmller, V., Dye, S.R., Skjoldal, H.R., 2008. Climate change and deepening of the North Sea fish assemblage: a biotic indicator of warming seas. J. Appl. Ecol. 45, 1029–1039.

Fang, E.J., Yu, J., Li, W.W., Mi, H.Q., Chen, W., 2011. Species composition and quantity distribution of floating eggs and juvenile fish in Bohai Bay. China Fisheries 60–62.

Ferreyro, B.L., Angriman, F., Munshi, L., Del Sorbo, L., Ferguson, N.D., Rochwerg, B., Ryu, M.J., Saskin, R., Wunsch, H., da Costa, B.R., Scales, D.C., 2020. Association of Noninvasive Oxygenation Strategies With All-Cause Mortality in Adults With Acute

Hypoxemic Respiratory Failure: A Systematic Review and Meta-analysis. J. Am. Med. Assoc. 324, 57–67.
Forrest, B.M., Taylor, M.D., 2002. Assessing invasion impact: survey design considerations and implications for management of an invasive marine plant. Biol. Invasions 12.
Forsberg, J.A., Dorsett, P.W., Neill, W.H., 1996. Survival and Growth of Red Drum Sciaenops ocellatus in Saline Groundwaters of West Texas. USA 27, 462–474.
Fossheim, M., Primicerio, R., Johannesen, E., Ingvaldsen, R.B., Aschan, M.M., Dolgov, A. V., 2015. Recent warming leads to a rapid borealization of fish communities in the Arctic. Nat. Clim. Chang. 5, 673–677.
Gaither, M.R., Aeby, G., Vignon, M., Meguro, Y., Rigby, M., Runyon, C., Toonen, R.J., Wood, C.L., Bowen, B.W., 2013. An invasive fish and the time-lagged spread of its parasite across the Hawaiian archipelago. PLoS One 8, e56940.
Geraldi, N.R., Anton, A., Lovelock, C.E., Duarte, C.M., 2019. Are the ecological effects of the "worst" marine invasive species linked with scientific and media attention? PLoS One 14, e0215691.
Gold, J.R., Burridge, C.P., Turner, T.F., 2001. A modified stepping-stone model of population structure in red drum, Sciaenops ocellatus (Sciaenidae), from the northern Gulf of Mexico. Genetica 111, 305–317.
Hill, J.E., 2009. Risk analysis for non-native species in aquaculture. Southern Regional Aquaculture Center (SRAC). Publication No. 4304.
Hixon, M.A., Green, S.J., Albins, M.A., Akins, J.L., Morris, J.A., 2016. Lionfish: a major marine invasion. Mar. Ecol. Prog. Ser. 558, 161–165.
Hollenbeck, C.M., Portnoy, D.S., Gold, J.R., 2019. Evolution of population structure in an estuarine-dependent marine fish. Ecol. Evol. 9, 3141–3152.
Holt, J.G., 1993. Feeding larval red drum on microparticulate diets in a closed recirculating water system. J. World Aquacult Soc. 24, 6.
Hu, X.G., Jin, Y., Wang, X.R., Mao, J.F., Li, Y., 2015. Predicting Impacts of Future Climate Change on the Distribution of the Widespread Conifer Platycladus orientalis. PLoS One 10, e0132326.
Hughes, I.I., 2000. Biological consequences of global warming: is the signal already apparent? Trends Ecol. Evol. 15, 56–61.
Jaafar, Z., Yeo, D.C.J., Tan, H.H., O'Riordan, R.M., 2012. Status of estuarine and marine non-indigenous species in Singapore. The. Raffles Bulletin of Zoology 13.
Jennings, S., Greenstreet, S., Hill, L., Piet, G., Pinnegar, J., Warr, K., 2002. Long-term trends in the trophic structure of the North Sea fish community: evidence from stable-isotope analysis, size-spectra and community metrics. Mar. Biol. 141, 1085–1097.
Ji, W.W., Chen, X.Z., Jiang, Y.Z., Liu, Y., Hu, F., Li, S.F., 2011. Stable isotope analysis of some representative nektonic organisms in the central and northern part of East China Sea. Marine Fisheries 33, 241–250.
Jin, H.W., Xu, H.X., Xu, W.J., Xue, L.J., 2008. Study on feeding habits Sciaenops ocellatus of the escaped red drum in Zhejiang sea area. Marine Fisheries Res. 29, 103–108.
Ju, R.T., Li, X., Jiang, J.J., Wu, J., Liu, J., Strong, D.R., Li, B., Knutie, S., 2019. Emerging risks of non-native species escapes from aquaculture: Call for policy improvements in China and other developing countries. J. Appl. Ecol. 57, 85–90.
Kang, B., Huang, X., Li, J., Liu, M., Guo, L., Han, C.-C., 2017. Inland Fisheries in China: Past, Present, and Future. Rev. Fish. Sci. Aquacult. 25, 270–285.
Kang, B., Vitule, J.R.S., Li, S., Shuai, F., Huang, L., Huang, X., Fang, J., Shi, X., Zhu, Y., Xu, D., Yan, Y., Lou, F., 2022. Introduction of non-native fish for aquaculture in China: A systematic review. Rev. Aquac. 1–28.
Kleisner, K.M., Fogarty, M.J., McGee, S., Hare, J.A., Moret, S., Perretti, C.T., Saba, V.S., 2017. Marine species distribution shifts on the US Northeast Continental Shelf under continued ocean warming. Prog. Oceanogr. 153, 24–36.
Langbehn, T.J., Varpe, Ø., 2017. Sea-ice loss boosts visual search: fish foraging and changing pelagic interactions in polar oceans. Glob. Chang. Biol. 23, 5318–5330.
Layman, C.A., Arrington, D.A., Montaña, C.G., Post, D.M., 2007. Can stable isotope ratios provide for community-wide measures of trophic structure? Ecology 88, 42–48.
Liang, M., Liang, P.D., Fan, L.L., Xu, J.J., 2022. Relationship between tropical cyclone scale and intensity over the Northwest Pacific from 1980 to 2016. Journal of Guangdong Ocean University 42, 8.
Liao, Y.C., Chen, L.S., Shao, K.T., 2010. The predatory Atlantic red drum, Sciaenops ocellatus, has invaded the western Taiwanese coast in the Indo-West Pacific. Biol. Invasions 12, 1961–1965.
Lin, B.A., Wang, Y.W., Li, J.L., Kang, B., Fang, L.P., Zheng, L.M., Liu, M., 2020. First records of small juveniles of the red drum Sciaenops ocellatus (Linnaeus, 1766) in a subtropical mangrove habitat of China. BioInvasions Records 9, 96–102.
Liu, D., Ma, Q., Valiela, I., Anderson, D.M., Keesing, J.K., Gao, K., Zhen, Y., Sun, X., Wang, Y., 2020. Role of C(4) carbon fixation in Ulva prolifera, the macroalga responsible for the world's largest green tides. Commun Biol 3, 494.
Liu, J.H., Mao, X.H., Wang, W.X., Wang, B., 1998. A preliminary study on technique for fully artificial breeding of red drum Sciaenops ocellatus. Journal of Fishery Sciences of China 5, 4.
Liu, C., White, M., Newell, G., 2013. Selecting thresholds for the prediction of species occurrence with presence-only data. J. Biogeogr. 40, 778–789.
Liu, J., Xiao, Y.S., 2021. Progress in fish diversity pattern and evolution in the Indo-Pacific convergence region. Oceanologia Et Limnologia Sinica 52, 498–507.
Luque, G.M., Bellard, C., Bertelsmeier, C., Bonnaud, E., Genovesi, P., Simberloff, D., Courchamp, F., 2014. The 100th of the world's worst invasive alien species. Biol. Invasions 16, 981–985.
Mack, R.N., Simberloff, D., Mark Lonsdale, W., Evans, H., Clout, M., Bazzaz, F.A., 2000. Biotic Invasions: Causes, Epidemiology, Global Consequences, and Control. Ecol. Appl. 10, 689–710.
McKinney, M.L., Lockwood, J.L., 1999. Biotic homogenization: a few winners replacing many losers in the next mass extinction. Trends Ecol. Evol. 14, 450–453.
Melo-Merino, S.M., Reyes-Bonilla, H., Lira-Noriega, A., 2020. Ecological niche models and species distribution models in marine environments: A literature review and spatial analysis of evidence. Ecological Modelling 415.
Minagawa, M., Wada, E., 1984. Stepwise enrichment of 15N along food chains: Further evidence and the relation between δ15N and animal age. Geochim. Cosmochim. Acta 48, 1135–1140.
Miyake, Y., Wada, E., 1967. The abundance ratio of 15N/14N in marine environments. Rec Oceanogr Works Jpn 9, 37–53.
Montie, E.W., Kehrer, C., Yost, J., Brenkert, K., O'Donnell, T., Denson, M.R., 2016. Long-term monitoring of captive red drum Sciaenops ocellatus reveals that calling incidence and structure correlate with egg deposition. J. Fish Biol. 88, 1776–1795.
Padilla, D.K., Williams, S.L., 2004. Beyond ballast water: aquarium and ornamental trades as sources of invasive species in aquatic ecosystems. Front. Ecol. Environ. 2, 131–138.
Parker, I.M., Simberloff, D., Lonsdale, W.M., Goodell, K., Wonham, M., Kareiva, P.M., Williamson, M.H., Von Holle, B., Moyle, P.B., Byers, J.E., Goldwasser, L., 1999. Impact: Toward a Framework for Understanding the Ecological Effects of Invaders. Biol. Invasions 1, 3–19.
Peake, J., Bogdanoff, A.K., Layman, C.A., Castillo, B., Reale-Munroe, K., Chapman, J., Dahl, K., Patterson Iii, W.F., Eddy, C., Ellis, R.D., Faletti, M., Higgs, N., Johnston, M. A., Muñoz, R.C., Sandel, V., Villasenor-Derbez, J.C., Morris, J.A., 2018. Feeding ecology of invasive lionfish (Pterois volitans and Pterois miles) in the temperate and tropical western Atlantic. Biol. Invasions 20, 2567–2597.
Pearce, J., Ferrier, S., 2000. An evaluation of alternative algorithms for fitting species distribution models using logistic regression. Ecol. Model. 128, 127–147.
Perry, A.L., Low, P.J., Ellis, J.R., Reynolds, J.D., 2005. Climate change and distribution shifts in marine fishes. Science (New York, N.Y.) 308, 1912-1915.
Peterson, C.H., 1993. Improvement of environmental impact analysis by application of principles derived from manipulative ecology: Lessons from coastal marine case histories. Austral Ecol. 18, 21–52.
Peterson, B.J., Fry, B., 1987. Stable isotopes in ecosystem studies. Annu. Rev. Ecol. Syst. 18, 293–320.
Phillips, S.J., Dudík, M., 2008. Modeling of species distributions with Maxent: new extensions and a comprehensive evaluation. 31, 161-175.
Phillips, S.J., Anderson, R.P., Schapire, R.E., 2006. Maximum entropy modeling of species geographic distributions. Ecol. Model. 190, 231–259.
Phillips, S.J., Anderson, R.P., Dudík, M., Schapire, R.E., Blair, M.E., 2017. Opening the black box: an open-source release of Maxent. 40, 887-893.
Picapedra, P.H.S., Sanches, P.V., Lansac-Toha, F.A., 2018. Effects of light-dark cycle on the spatial distribution and feeding activity of fish larvae of two co-occurring species (Pisces: Hypophthalmidae and Sciaenidae) in a Neotropical floodplain lake. Braz. J. Biol. 78, 763–772.
Pimentel, D., Lach, L., Zuniga, R., Morrison, D., 2000. Environmental and economic costs of nonindigenous species in the United States. BioScienc 50, 53–65.
Pimentel, D., Zuniga, R., Morrison, D., 2005. Update on the environmental and economic costs associated with alien-invasive species in the United States. Ecol. Econ. 52, 273–288.
Ponton, D.E., Lavoie, R.A., Leclerc, M., Bilodeau, F., Planas, D., Amyot, M., 2021. Understanding Food Web Mercury Accumulation Through Trophic Transfer and Carbon Processing along a River Affected by Recent Run-of-river Dams. Environ. Sci. Tech. 55, 2949–2959.
Post, D.M., 2002. Using Stable Isotopes to Estimate Trophic Position: Models, Methods, and Assumptions. Ecology 83, 703–718.
Potts, W.M., Henriques, R., Santos, C.V., Munnik, K., Ansorge, I., Dufois, F., Booth, A.J., Kirchner, C., Sauer, W.H., Shaw, P.W., 2014. Ocean warming, a rapid distributional shift, and the hybridization of a coastal fish species. Glob. Chang. Biol. 20, 2765–2777.
Qin, C., Chen, P., Sarà, G., Mo, B., Zhang, A., Li, X., 2020. Ecological implications of purple sea urchin (Heliocidaris crassispina, Agassiz, 1864) enhancement on the coastal benthic food web: evidence from stable isotope analysis. Mar. Environ. Res. 158, 104957.
Robinson, L.M., Elith, J., Hobday, A.J., Pearson, R.G., Kendall, B.E., Possingham, H.P., Richardson, A.J., 2011. Pushing the limits in marine species distribution modelling: lessons from the land present challenges and opportunities. Glob. Ecol. Biogeogr. 20, 789–802.
Robinson, N.M., Nelson, W.A., Costello, M.J., Sutherland, J.E., Lundquist, C.J., 2017. A Systematic Review of Marine-Based Species Distribution Models (SDMs) with Recommendations for Best Practice. Front Mar Sci 4.
Rooker, J.R., Stunz, G.W., Holt, S.A., Minello, T.J., 2010. Population connectivity of red drum in the northern Gulf of Mexico. Mar. Ecol. Prog. Ser. 407, 187–196.
Sala, O.E., Chapin, F.S., 3rd, Armesto, J.J., Berlow, E., Bloomfield, J., Dirzo, R., Huber-Sanwald, E., Huenneke, L.F., Jackson, R.B., Kinzig, A., Leemans, R., Lodge, D.M., Mooney, H.A., Oesterheld, M., Poff, N.L., Sykes, M.T., Walker, B.H., Walker, M., Wall, D.H., 2000. Global biodiversity scenarios for the year 2100. Science (New York, N.Y.) 287, 1770-1774.
Sancho, G., Kingsley-Smith, P.R., Morris, J.A., Toline, C.A., McDonough, V., Doty, S.M., 2018. Invasive Lionfish (Pterois volitans/miles) feeding ecology in Biscayne National Park, Florida, USA. Biol. Invasions 20, 2343–2361.
Sandø, A.B., Johansen, G.O., Aglen, A., Stiansen, J.E., Renner, A.H.H., 2020. Climate Change and New Potential Spawning Sites for Northeast Arctic cod. Front. Mar. Sci. 7, 28.
Smith, S.D., Huxman, T.E., Zitzer, S.F., Charlet, T.N., Housman, D.C., Coleman, J.S., Fenstermaker, L.K., Seemann, J.R., Nowak, R.S., 2000. Elevated CO2 increases productivity and invasive species success in an arid ecosystem. Nature 408, 79–82.
Tatem, A.J., Hay, S.I., Rogers, D.J., 2006. Global traffic and disease vector dispersal. Proc. Natl. Acad. Sci. U.S.A. 103, 6242–6247.

Thresher, R.E., Kuris, A.M., 2004. Options for Managing Invasive Marine Species. Biol. Invasions 6, 295–300.
Tu, Q.Y., Shi, Q.W., Lin, Y.X., Wang, W.X., 2002. Case report: Ovine flagellate and xenomorphic trematode infection of Sciaenops ocellatus. Taiwan J. Veterin. 28, 7.
Turner, T.F., Richardson, L.R., Gold, J.R., 1999. Temporal genetic variation of mitochondrial DNA and the female effective population size of red drum (Sciaenops ocellatus) in the northern Gulf of Mexico. Mol. Ecol. 8, 1223–1229.
Uyan, U., Oh, C.-W., Tarkan, A.S., Top, N., Copp, G.H., Vilizzi, L., 2020. Risk screening of the potential invasiveness of non-native marine fishes for South Korean coastal waters. Mar. Pollut. Bull. 153, 111018.
Vander Zanden, M., Vadeboncoeur, Y., 2002. Fishes as integrators of benthic and pelagic food webs in lakes. J. Ecology 83, 2152–2161.
Walther, G.R., Roques, A., Hulme, P.E., Sykes, M.T., Pysek, P., Kühn, I., Zobel, M., Bacher, S., Botta-Dukát, Z., Bugmann, H., Czúcz, B., Dauber, J., Hickler, T., Jarosík, V., Kenis, M., Klotz, S., Minchin, D., Moora, M., Nentwig, W., Ott, J., Panov, V.E., Reineking, B., Robinet, C., Semenchenko, V., Solarz, W., Thuiller, W., Vilà, M., Vohland, K., Settele, J., 2009. Alien species in a warmer world: risks and opportunities. Trends Ecol. Evol. 24, 686–693.
Wang, B., Zhang, X.L., 1998. Research on the net tank culture technology of Sciaenops ocellatus. South China Sea Res. Dev. 5.
Wang, H.J., Zhang, W.B., Huang, H.H., Xu, S.N., Liu, H.X., 2021. Trophic structure of fishery organism assemblage in Daya Bay based on carbon and nitrogen stable isotope analysis. South China Fisheries Science 17, 101–109.
Wang, X., Zhang, H., Lu, G., Gao, T., 2022. Detection of an invasive species through an environmental DNA approach: The example of the red drum Sciaenops ocellatus in the East China Sea. Sci. Total Environ. 815, 152865.
Warren, D.L., Glor, R.E., Turelli, M., 2010. ENMTools: a toolbox for comparative studies of environmental niche models. Ecography 607–611.
Watson, C.J., Nordi, W.M., Esbaugh, A.J., 2014. Osmoregulation and branchial plasticity after acute freshwater transfer in red drum, Sciaenops ocellatus. Comp. Biochem. Physiol. A Mol. Integr. Physiol. 178, 82–89.
Williamson, M., Fitter, A., 1996. The Varying Success of Invaders. Ecology 77, 1661–1666.
Xu, K.D., 2021. Formation and evolution mechanisms of marine biodiversity center in the Indo-Pacific convergence region: progress and prospects. Oceanologia Et Limnologia Sinica 52, 262–273.
Xue, L.J., 2008. Elementary study on the influence of the escaping net breeded Sciaenops ocellatus on natural zoology of Zhejiang sea area. Ocean University of China.
Yan, Y.R., Zhang, W.K., Lu, H.S., Wang, X.F., Lai, J.Y., 2012. Using stable isotopes to analyze feeding habits and trophic position of hairtail (Trichiurus lepturus) from the beibu gulf, South China Sea. Oceanologia Et Limnologia Sinica 43, 192–200.
Yin, C., 2020. Tropical cyclone induced storm wave hazard assessment in Hainan Island. University of Chinese Academy of Sciences, China.
Zhang, B., Ma, N.F., Jiang, Z.Q., 2002. Pond Cultural Technique of Sciaenops Ocellatus. 21, 2.
Zhang, Z., Mammola, S., Zhang, H., 2020. Does weighting presence records improve the performance of species distribution models? A test using fish larval stages in the Yangtze Estuary. Sci. Total Environ. 741, 140393.